

Open charm production in relativistic nucleus-nucleus collisions *

W. Cassing, E. L. Bratkovskaya, A. Sibirtsev

Institut für Theoretische Physik,
Universität Giessen, 35392 Giessen, Germany

Abstract

We calculate excitation functions for open charm mesons in $Au + Au$ reactions from AGS to RHIC energies within the HSD transport approach which is based on string, quark, diquark ($q, \bar{q}, qq, \bar{q}\bar{q}$) and hadronic degrees of freedom. The open charm cross sections from pN and πN reactions are fitted to results from PYTHIA and scaled in magnitude to the available experimental data. From our dynamical calculations we find an m_T -scaling for pions, kaons, D -mesons and J/Ψ – when discarding final state elastic scattering of kaons and ϕ -mesons with pions – in central collisions of $Au + Au$ at 160 A·GeV (with an apparent slope of 176 MeV) without employing the assumption of a Quark-Gluon Plasma (QGP). We demonstrate that this result is essentially due to an approximate m_T -scaling in pp collisions at $\sqrt{s} \approx 17.3$ GeV. At lower bombarding energies of 25 A·GeV a suppression of D -mesons by a factor of ~ 10 relative to a global m_T -scaling with slope 143 MeV is expected. However, when incorporating attractive D -meson self energies as suggested by QCD sum rules, an approximate m_T -scaling is regained even at 25 A·GeV. The effects of D -meson rescattering and charmonium absorption are discussed, furthermore, with respect to rapidity and transverse mass distributions in central collisions of $Au + Au$ at 25 and 160 A·GeV.

PACS: 25.75.-q; 13.60.L2; 14.40.Lb; 14.65.Dw

Keywords: Relativistic heavy-ion collisions; Meson production; Charmed mesons; Charmed quarks

*supported by GSI Darmstadt and FZ Jülich

1 Introduction

Apart from the light and strange flavor ($u, \bar{u}, d, \bar{d}, s, \bar{s}$) quark physics and their hadronic bound states in the vacuum (π, K, ϕ etc.) the interest in hadronic states with charm flavors (c, \bar{c}) has been rising continuously in line with the development of new experimental facilities [1, 2, 3, 4]. This relates to the charm production cross section in pN and πN reactions as well as to their interactions with baryons and mesons which determine their properties (spectral functions) in the hadronic medium.

The charm quark degrees of freedom have gained vivid interest especially in the context of a phase transition to the quark-gluon plasma (QGP) [5] where $c\bar{c}$ meson states should no longer be formed due to color screening [6, 7]. However, the suppression of J/Ψ and Ψ' mesons in the high density phase of nucleus-nucleus collisions [8, 9] might also be attributed to inelastic comover scattering (cf. [10, 11, 12, 13, 14, 15] and Refs. therein) provided that the corresponding J/Ψ -hadron cross sections are in the order of a few mb [16, 17, 18, 19, 20, 21]. Present theoretical estimates here differ by more than an order of magnitude [22] especially with respect to J/Ψ -meson scattering such that the question of charmonium suppression is not yet settled. On the other hand, the enhancement of 'intermediate-mass dileptons' in $Pb + Pb$ collisions at the SPS has been tentatively attributed to an enhancement of 'open charm' in nucleus-nucleus collisions relative to pA reactions at the same invariant energy \sqrt{s} [23]. It should be mentioned that this enhancement does not stem from the charmonium dissociation since it is about two orders of magnitude larger the total charmonium yield. Thus 'charmonium suppression' and 'open charm enhancement' are present facets of relativistic heavy-ion collisions.

Furthermore, it is well known experimentally [24] that the D, \bar{D} and D^*, \bar{D}^* mesons show some analogy to the K, \bar{K} and K^*, \bar{K}^* mesons with respect to their excitation spectrum because the strange (antistrange) quark is replaced by a charm (anticharm) quark in the hadronic state. Since quite substantial in-medium potentials have been suggested for antikaons in dense nuclear matter [10, 25], the latter might also show up for the corresponding D -mesons in view of a similar wavefunction for the light quark [26]. In fact, QCD sum rule studies point towards attractive potentials for the D -mesons [27] which might lead to enhanced production cross sections of open charm especially at low bombarding energies close to threshold. Substantially lower in-medium effects are expected for the J/Ψ or η_c do to a small coupling of the c, \bar{c} quarks to the nuclear medium [28]. Thus the charm-meson sector, which is insufficiently known so far, provides a theoretical [19, 29, 30, 31, 32, 33] and experimental challenge for the future [34, 35].

In this work we will explore the perspectives for open charm production in nucleus-collisions from AGS to RHIC energies employing the HSD transport approach [10, 14] for the overall reaction dynamics using parametrizations for the elementary production channels including the charmed hadrons $D, \bar{D}, D^*, \bar{D}^*, D_s, \bar{D}_s, D_s^*, \bar{D}_s^*, J/\Psi, \Psi(2S), \chi_{2c}$ from NN and πN collisions. The latter parametrizations are fitted to PYTHIA calculations [36] above $\sqrt{s} = 10$ GeV and extrapolated to the individual thresholds, while the absolute strength of the cross sections is fixed by the experimental data [37, 38, 39, 40, 41, 42, 43, 44, 45, 46, 47] similar to Ref. [30].

We recall that in the HSD transport approach the initial stages of a pp , pA or AA reaction (at high energy) are described by the excitation of color neutral strings, where the

leading quarks and 'diquarks' in a baryonic string (or quarks and antiquarks in a mesonic string etc.) are allowed to rescatter again (in pA and AA collisions) with hadronic cross sections divided by the number of constituent quarks and antiquarks in the hadrons, respectively [49]. We, furthermore, note that the underlying LUND model [50] includes partonic diffractive scattering and mini-jet production as well [36]. The latter phenomena are not important at SPS energies and below, however, become appreciable at RHIC energies. In this respect the HSD approach dynamically also includes the hard partonic processes as far as quarks and antiquarks are involved. However, it does not employ hard gluon-gluon processes beyond the level of 'string phenomenology'. This has to be kept in mind with respect to the validity of the model at RHIC energies; for more detailed predictions at the highest energies we refer the reader to Ref. [14]. Here we concentrate on open charm and charmonium physics at 25 and 160 A·GeV, respectively.

2 Elementary cross sections from pN and πN collisions

Before examining nucleus-nucleus collisions we have to specify the differential open charm cross sections from pN and πN reactions that will enter the HSD approach. Contrary to light meson production in hadronic reactions the creation of a $c\bar{c}$ pair is due to a hard process and dominated by gluon-gluon fusion. Using MRS G (next to leading order) structure functions from the PDFLIB package [51] for the gluon distribution of the proton, a bare charm quark mass $m_c = 1.5$ GeV and $k_T = 1$ GeV we obtain the cross sections for $D, \bar{D}, D^*, \bar{D}^*, D_s, \bar{D}_s, D_s^*, \bar{D}_s^*$, as a function of $\sqrt{s} \geq 10$ GeV from PYTHIA [36] as displayed in Fig. 1 (upper part). Corresponding results for πN reactions are shown in the lower part. Since the individual lines are hard to distinguish, some general trends are pointed out: All cross sections indicate a common (smooth) energy dependence. The D^* -mesons are created more abundantly than the D -mesons roughly by a factor of 3 due to the three different spin polarizations; the small mass difference between D - and D^* -mesons of ≈ 140 MeV plays almost no role above $\sqrt{s} \geq 10$ GeV. On the other hand, an exchange of a light (u, d) quark by a strange (s) quark costs a factor of 3-4. Consequently, the cross sections of D^0, \bar{D}^0, D^+, D^- and D_s^*, \bar{D}_s^* are roughly comparable at high \sqrt{s} . These simple considerations specify the relative abundance of the open charm mesons. However, the absolute magnitude of the cross sections is not expected to match experimental data due to the perturbative nature of these calculations and rescaling factors K have to be introduced [30].

In this spirit we fit the individual results from PYTHIA (multiplied by factors of 12 and 7 for pN and πN , respectively) by an expression of the form,

$$\sigma_X(s) = a_X(1 - Z)^\alpha Z^{-\beta}, \quad (1)$$

with $Z = \sqrt{s_X^0}/\sqrt{s}$ where $\sqrt{s_X^0}$ denotes the threshold for the channel X in pN or πN reactions. Note that close to threshold the production for $D(\bar{c})$ -mesons is enhanced relative to $D(c)$ -mesons since the c -quark can end up in $\Lambda_c, \Sigma_c, \Sigma_c^*$ baryons with lower threshold. $D(c)$ -mesons require the associated production with a $D(\bar{c})$ meson. These threshold phenomena are in close analogy to the strangeness sector where the mesons with a \bar{s} -quark are

produced close to threshold essentially together with hyperons (Λ, Σ) whereas antikaons require the associated production with a kaon.

The formula (1) ensures the proper thresholds by construction while the exponents α and β describe the rise at threshold and the asymptotic behaviour, respectively. In order to properly 'normalize' the results from Fig. 1 we address to the experimental data from Refs. [37, 38, 39, 40, 41, 42, 43, 44, 45, 46, 47] that have been extrapolated to full open charm cross sections by using the charge ratio's as given by PYTHIA. Furthermore, we have used a factor of 2 when extrapolating data for $x_F > 0$ to the full Feynman x_F regime for pN collisions and a factor of 1.6 for πN reactions [52]. The results of the fits are given in Tables 1 and 2 for the parameters a_X, α and β . We mention that the high value of the exponent α compared to related fits for ρ, ω or ϕ production [10] indicates the different production mechanism for $c\bar{c}$ pairs compared to light quark pairs.

The parametrized results from this extrapolation are displayed in Fig. 2 for pN (upper part) and πN reactions (lower part) for the full charm cross section including all mesons as specified above with their individual thresholds. The solid lines in Fig. 2 represent the sum over all open charm mesons (within the parameters given in Tables 1 and 2) while the individual lines refer to the individual mesons that are somewhat hard to disentangle. As in Fig. 1 these cross sections group to 3 bunches at high \sqrt{s} where the upper bundle of lines corresponds to D^{*+}, D^{*-}, D^{*0} and \bar{D}^{*0} , the middle bundle to D^+, D^-, D^0, \bar{D}^0 and the vector states with a strange quark D_s^*, \bar{D}_s^* , while the lower bundle gives the cross section for D_s, \bar{D}_s .

It is interesting to compare these results with the cross sections for J/Ψ (including χ_c decay) and Ψ' ($\Psi(2S)$) which are displayed in Fig. 3 as a function of \sqrt{s} together with the parametrizations (solid lines) for pN and πN reactions (taken from Ref. [11, 48]). Note that at $\sqrt{s} = 20$ GeV open charm is enhanced by about a factor of 50 relative to J/Ψ and that this ratio increases with the available energy. Since the parametrization from Ref. [48] approaches some constant value at high \sqrt{s} contrary to the PYTHIA calculations (cf. Fig. 1 of Ref. [11]) we have fitted the total cross section by the function

$$\sigma_X(s) = b_X(1 - Y)^\alpha Y^{-\beta} \Theta(\sqrt{s} - \sqrt{s_0}) \quad (2)$$

with $Y = m_X/\sqrt{s}$ and $\alpha = 10$, while $\sqrt{s_0}$ denotes the threshold in vacuum. Again the parameter β governs the high energy rise of the cross section which for $\beta \approx 1$ is now in line with the PYTHIA calculations specified above. Our fits give $b_{J/\Psi} = 96$ nb, $b_{\chi_c} = 64$ nb, $b_{\Psi'} = 20$ nb; the results for J/Ψ (including the χ_c decay) are shown in the upper part of Fig. 3 in terms of the dashed line.

The cross sections (1),(2) will be used in the transport calculations to be discussed below which, apart from the total cross sections, also need the differential distribution of the produced mesons in the transverse momentum p_T and the rapidity y (or Feynman x_F) from each individual collision. We recall that $x_F = p_z/p_z^{max} \approx 2p_z/\sqrt{s}$ with p_z denoting the longitudinal momentum. For the differential distribution in x_F and p_T we use the ansatz,

$$\frac{dN}{dx_F dp_T^2} \sim (1 - |x_F|)^\gamma \exp(-bp_T^2), \quad (3)$$

with $\gamma \approx 4.5$ and $b = 1$ GeV⁻². With these parameters the differential transverse momentum distributions of D/\bar{D} mesons in pp (and πN) reactions at 250 GeV [45] may

reasonably be described as shown in Fig. 4 at least up to $6 \text{ GeV}^2/c^2$. At higher transverse momenta there is an indication for a component $\sim \exp(-b_2 p_T)$ that could be added to (3), however, we neglect such a component to keep the numbers of parameters as low as possible. The x_F and p_T distribution for charmonium production, furthermore, is taken from Ref. [53].

We have to point out that our parametrizations for the differential and total cross sections for open charm (as well as charmonia) become questionable at low energy, but also at high energy. It is thus mandatory that they have to be controlled by experimental data from pp , pA and πN reactions before reliable conclusions on open charm dynamics in nucleus-nucleus reactions can be drawn.

For the interpretation of the results from nucleus-nucleus collisions (cf. Section 3) it is worth to compare to pp collisions at different energies, respectively. To this aim we display in Figs. 5–7 the differential multiplicities $(2m_T)^{-1} dN_X/dm_T$ in the transverse mass

$$m_T = \sqrt{p_T^2 + m_X^2} \quad (4)$$

for all final pions, kaons, ϕ -mesons, $D + \bar{D}$ mesons and charmonia from pp reactions at $\sqrt{s} = 7.1 \text{ GeV}$, 17.3 GeV and 200 GeV , respectively. The pion spectra describe the sum of π^+, π^0, π^- , the kaon spectra the sum of K^+, K^0, \bar{K}^0, K^- , the D -meson spectra the sum of all D, D^*, D_s, D_s^* and their antiparticles while the spectrum denoted by $c\bar{c}$ includes the J/Ψ , the χ_c as well as the Ψ' which becomes visible as a tiny kink in the m_T -spectra at $m_T \approx 3.7 \text{ GeV}$. Here the open charm and charmonia results stem from the parametrizations specified above (including the decay $\chi_c \rightarrow J/\Psi + \gamma$) while the spectra for pions, kaons and ϕ -mesons are from the LUND string model [50] (as implemented in the HSD transport approach). For orientation we also show exponential spectra with slope parameters of 143 MeV , 176 MeV and 225 MeV , respectively, which describe the m_T -spectra of pions rather well. The kaon spectra at all energies are down by a factor of ~ 3 , the ϕ spectra by a factor of 9–10 relative to this line due to strangeness suppression in pp collisions. However, it is quite remarkable that the charmonia spectra fit well to this m_T -scaling (within a factor of 2–3) at $\sqrt{s} = 7.1, 17.3$ and 200 GeV , respectively. Furthermore, the spectrum of open charm is roughly compatible with m_T -scaling at $\sqrt{s} = 17.3$ and 200 GeV , while the D, \bar{D} mesons are suppressed relative to the scaling by a factor ~ 50 close to threshold ($\sqrt{s} = 7.1 \text{ GeV}$). Whereas these results basically stem from our parametrizations at $\sqrt{s} = 7.1$ and 200 GeV , the spectra at $\sqrt{s} = 17.3$ are controlled by experimental data. The 'apparent' statistical production of mesons in elementary reactions has been advocated before by Becattini [54].

We point out that also the m_T -scaling from Figs. 5–7 has to be controlled by explicit experimental measurements. Data in a limited rapidity range might lead to somewhat different results since the rapidity distributions of pions, kaons, ϕ 's, D 's, D^* 's and charmonia differ substantially due to kinematical reasons.

3 Nucleus-nucleus collisions

Inspite of the inherent uncertainties pointed out above it is worthwhile to explore the dynamics of open charm mesons in relativistic nucleus-nucleus collisions. Experiments

are planned at the SPS [34] and might be even performed in the 20–30 A·GeV region [55]. Here we will employ the HSD transport approach for the nucleus-nucleus dynamics that has been tested in detail for pp , pA and AA reactions from SIS to SPS energies [10] and been used for the description of charmonium production and propagation as well [14, 56, 57].

We recall that (as in Refs. [56, 57]) the charm degrees of freedom are treated perturbatively and that hard process (such as $c\bar{c}$ or Drell-Yan production) are 'precalculated' to achieve a scaling of the inclusive cross section with the number of projectile and target nucleons as $A_P \times A_T$. To implement this scaling we separate the production of the hard and soft processes: The space-time production vertices of the $c\bar{c}$ pairs are calculated in each transport run by neglecting the soft processes, i.e. the production of light quarks and associated mesons. The resulting number $N_{coll}(b)$ of these 'hard' collisions is shown for $Au + Au$ at 160 A·GeV in Fig. 8 (full squares) as a function of impact parameter. The inclusive number of inelastic NN collisions is given by the integral of N_{coll} over impact parameter

$$I = \frac{2\pi \int b N_{coll}(b) db}{\sigma_{inel.}(\sqrt{s})} \approx A^2, \quad (5)$$

which gives approximately A^2 , i.e. the experimental scaling for 'hard' processes. In (5) the mass number $A = 197$ for Au , while $\sigma_{inel.}(\sqrt{s})(\approx 34 \text{ mb})$ denotes the inelastic nucleon-nucleon cross section. The calculated $N_{coll}(b)$ compares well with the result from Glauber theory (solid line in Fig. 8), where the number of inelastic interactions in nucleus-nucleus collision $A+B$ at impact parameter $\mathbf{b} = (b, 0, 0)$ is given as [58, 59]

$$N_{AB}(b) = A B \int \sigma_{inel} T_A(\mathbf{s}) T_B(\mathbf{s} - \mathbf{b}) d^2 s, \quad (6)$$

where $\mathbf{s} = (s_x, s_y, 0)$ is orthogonal to the z -direction. In the integral (6)

$$T_A(b) = \int_{-\infty}^{+\infty} \rho(\sqrt{b^2 + z^2}) dz \quad (7)$$

is the profile function normalized to unity, while $\rho(r)$ is the nuclear density taken of Woods-Saxon shape.

Thus the scaling of hard processes is adequately realized in the transport approach. We mention that this scaling prescription might no longer be valid at low and high energy due to modifications of the gluon structure functions during the heavy-ion reaction or related shadowing phenomena [60]. For our initial study, however, we discard such effects.

In the transport calculation we follow the motion of the charmonium pairs or produced D, \bar{D} -mesons within the full background of strings/hadrons by propagating them as free particles, i.e. neglecting in-medium potentials¹, but follow their collisional history with baryons and mesons or quarks and diquarks. For reactions with diquarks we use the corresponding reaction cross section with baryons multiplied by a factor of 2/3. For collisions with quarks (antiquarks) we adopt half of the cross section for collisions with

¹Except for the case of in-medium mass shifts in Section 3.2

mesons. Whereas the latter concept is oriented at the additive quark model, this assumption still does not solve the problem since the cross sections of D -mesons or charmonia with baryons and various mesons (essentially π , ρ and ω mesons) are not well known. Thus we will provide results with and without rescattering of open charm mesons.

In order to study the effect of rescattering we tentatively adopt the following dissociation cross sections of charmonia with baryons independent on the energy:

$$\sigma_{c\bar{c}B} = 6 \text{ mb}; \quad \sigma_{J/\Psi B} = 4 \text{ mb}; \quad \sigma_{\chi_{cB}} = 5 \text{ mb}; \quad \sigma_{\Psi'B} = 10 \text{ mb}, \quad (8)$$

while a lifetime (in it's rest frame) of 0.4 fm/c is assumed for the pre-resonance $c\bar{c}$ pair [61]. The energy-dependent J/Ψ -meson cross sections for dissociation to $D\bar{D}$ are taken from the calculations of Haglin [16] which on average lead to a similar J/Ψ comover suppression than the overall cross section of 3 mb adopted in Ref. [56].

On the other hand, the D/\bar{D} mesons are expected to have large cross sections with mesons or baryons due to the light flavor content such that light meson (π, ρ, ω, η) exchanges should describe the dominantly elastic cross sections at low relative momenta. We here adopt the calculations from Ref. [19] which predict elastic cross sections in the range of 10–20 mb for D, D^* scattering with mesons dependent on the size of the formfactor employed. As a guideline we use a constant cross section of 10 mb for elastic scattering with mesons and also baryons, although the latter might be even much higher for very low relative momenta. We neglect charm exchange reactions such as $D^+N \rightarrow \pi\Lambda_c, \Sigma_c$ or $\pi\Lambda_c \rightarrow \bar{D}N$ in the present study, which will essentially modify the charm quark content of mesons relative to baryons. Furthermore, we discard a recreation of charmonia by channels such as $D + \bar{D} \rightarrow J/\Psi + \pi$, since at AGS and SPS energies these reactions are negligible [30] whereas at RHIC energies this charmonium formation might become essential [31]. However, the formation cross sections are not well known and the significance of these channels is discussed controversially in the present literature [29, 31, 62].

In the transport calculations to be discussed below we will focus on the relative yield of pions, kaons, ϕ -, $D + \bar{D}$ -mesons and charmonia, that will be analyzed in terms of global m_T -spectra which are integrated over the whole rapidity range. In order to allow for a more direct comparison with the m_T -spectra from pN collisions in Figs. 5–7 we have 'switched off' a couple of reaction channels. The reason is as follows: The decay $\phi \rightarrow K\bar{K}, \pi\rho$ has been suppressed to allow for a direct evaluation of the ϕ -meson m_T -spectra at the end of the calculation. Furthermore, it is well known experimentally [1, 2, 3] that the apparent slope of m_T -spectra for different hadrons varies almost linearly with the hadron rest mass. This variation is attributed to a common collective flow velocity β and – in the transport calculations – results from elastic collisions between the hadrons in the expansion phase of the reaction [63]. In order to avoid ambiguities in the decomposition of the final spectra into a 'collective' and 'thermal' part (cf. the discussion in Section 3 of Ref. [63]) we have suppressed elastic collisions of kaons and ϕ -mesons in the expansion phase with pions ('pion wind'). This then leads to m_T -spectra with roughly the same slope for all hadrons (see below) and their relative abundance can be extracted in a simple way.

Note, however, that the calculated spectra should not directly be compared to experimental data in view of the suppression of elastic scattering processes. The modifications of the m_T -spectra due to the latter processes will be discussed in Section 3 separately.

3.1 SPS energies

We now turn to the results of transport calculations. In Fig. 9 we show the time evolution of c, \bar{c} production (solid line) for a central ($b = 1$ fm) collision of $Au + Au$ at 160 A·GeV in comparison to s, \bar{s} production (dashed line), where the c, \bar{c} number is scaled in height to the s, \bar{s} line for the initial 'hard' production by a factor of 1.5×10^3 . Both functions rise steeply within about 1 fm/c; whereas the solid line (c, \bar{c}) stays practically constant the dashed line (s, \bar{s}) increases smoothly due to secondary and ternary $s\bar{s}$ production by meson-baryon or meson-meson collisions [49]. This 'cooking' of strangeness in the expanding 'fireball' leads to a moderate (~ 46 %) enhancement of strangeness whereas the secondary production of $c\bar{c}$ pairs can be neglected at SPS energies. In this respect charm quark pairs are created in the initial high density phase of the collision with energy densities even above 3 GeV/fm³ [64]. The multiplicity of open charm mesons here is about 0.2, whereas the multiplicity of J/Ψ 's (including the decay of χ_c) is only about 10^{-3} . The fraction of charmonia dissociated by baryons and mesons is 70% for J/Ψ , 80 % for χ_c and 90 % for Ψ' , which is comparable to the suppression calculated earlier in Ref. [56].

The effect of rescattering of D -mesons on baryons and mesons as well as charmonium interactions with hadrons is shown in Fig. 10 for a central collision of $Au + Au$ with respect to the transverse mass spectra. Here the D, D^* spectrum is essentially flattened out in transverse mass while the charmonium spectrum is roughly reduced by a factor 3-4 due to dissociation reactions. We point out that a drastic enhancement of the slope of the D -meson m_T -spectra as advocated in Refs. [32, 33] is not seen from our dynamical calculations. Quite remarkably, the open charm spectra and charmonium spectra appear to scale in transverse mass after including the secondary interactions with hadrons. The effect of final state interactions on the rapidity distribution of D -mesons is displayed in Fig. 11 which shows a slight broadening of the distribution due to the elastic scattering processes.

It is interesting to have a look at the m_T -spectra for all mesons in analogy to Fig. 6 (for pp reactions) to explore the effects of open charm and charmonium rescatterings. The calculated m_T spectrum for pions, kaons, ϕ -mesons, all $D + \bar{D}$ mesons and charmonia is given in Fig. 12 which can be characterized well by an exponential slope parameter of 176 MeV (dashed line) for all mesons. This result comes about as follows when compared to Fig. 6: The D -mesons are created more abundantly than pions (relative to pp) in central collisions of $Au + Au$ because the D -meson (and charmonium) yield scales with the number of hard collisions (cf. Fig. 8) while the pions roughly scale with the number of participants and may be reabsorbed to some extent. The kaon (and ϕ) yield increases due to rescattering (cf. Fig. 9), however, the ϕ ($s\bar{s}$) mesons do not match the m_T -scaling in the HSD transport approach and stay down by a factor of about 3-4. The charmonium spectrum (relative to pp) is decreased by a factor $\approx 3-4$ due to dissociation processes as noted before. All these effects lead to the approximate m_T -scaling without employing the assumption of a Quark-Gluon Plasma (QGP) formation and a common hadronization at some temperature of 160 – 180 MeV.

We mention that a roughly constant π to J/Ψ ratio from pp to central $Pb+Pb$ collisions has been also pointed out in Refs. [65, 66] proposing a statistical hadronization scheme in all reactions. Furthermore, Gallmeister *et al.* have suggested in Ref. [67] that the open

charm degrees of freedom might be described in a simple thermodynamical model for central collisions of $Pb + Pb$ at the SPS using the same temperature for all mesons. The findings of these authors are supported here by the nonequilibrium transport calculations, that provide simple arguments for the phenomena pointed out before.

As mentioned above, the m_T -spectra from Fig. 12 should not be compared with experiment directly. Here the final state elastic scattering of kaons and ϕ -mesons with pions has to be taken into account which leads to a lowering of the pion slope parameter by a few % (due to pion 'cooling'), an enhancement of the kaon slope parameter by $\sim 25\%$ (due to an acceleration by the pions) and an enhancement of the ϕ -meson slope by about 20%. We note explicitly, that the high slope parameter for ϕ -mesons of ~ 300 MeV seen experimentally at midrapidity in central collisions of $Pb + Pb$ at the SPS by NA49 [68] is not reproduced within the HSD calculations due to the weak coupling of ϕ -mesons to non-strange hadrons. If this phenomenon is related to an early acceleration of strange quarks and antiquarks in a QGP phase or due to unexpected large rescattering cross sections is presently unclear.

3.2 $Au + Au$ reactions at 25 A·GeV

In this subsection we explore the perspectives of open charm measurements in nucleus-nucleus collisions at 25 A·GeV, which might be accessible at a possible future GSI facility [55]. In this initial study we restrict to central collisions of $Au + Au$ at 25 A·GeV, which is expected to provide the optimal conditions for open charm experiments and studies on the in-medium properties of D -mesons in analogy to the K^+, K^- experiments at the SIS. We step ahead as in Section 3.1.

Fig. 13 shows the time evolution of c, \bar{c} production (solid line) for a central ($b = 1$ fm) collision in comparison to s, \bar{s} production (dashed line) where the number of c, \bar{c} is scaled again in height to the s, \bar{s} line for the initial 'hard' production (by a factor 1.5×10^5). Both functions rise within a few fm/c which corresponds to the passage time of the (Lorentz contracted) nuclei. As in Fig. 9 the solid line (c, \bar{c}) stays constant for later times while the dashed line (s, \bar{s}) increases again due to secondary and ternary $s\bar{s}$ production channels. The relative enhancement of $s\bar{s}$ 'cooking' here amounts to roughly 65%. We note, however, that such an enhancement of strangeness is insufficient to explain the K^+ abundancies at the AGS [69] from 4 - 11 A·GeV or the K/π ratio at 40 A GeV (at the SPS) without assuming any in-medium modifications of the kaons. For a detailed discussion we refer the reader to Refs. [14, 49].

It is apparent from Fig. 13 that the charm quark pairs are created in the initial high density phase of the collision, here with energy densities up to 2 GeV/fm³, which is above the critical energy density from lattice calculations for the formation of a QGP [70]. However, the energy densities from the transport calculation correspond to nonequilibrium phase-space configurations at high baryon density, that should not be identified with the energy density extracted from lattice calculations (in equilibrium and for $\mu_q = 0$).

For a quantitative orientation we display in Fig. 14 the volume (in the nucleus-nucleus center-of-mass) with an energy density above 1 GeV/fm³ and 2 GeV/fm³ as a function of time for a central $Au + Au$ collision at 25 A·GeV, where only interacting and produced hadrons have been counted. It is important to note that the high energy

density is essentially build up from 'strings', i.e. 'unformed' hadrons. This phase has been addressed as *string matter* in Ref. [71] and expresses the notion that most of the hadrons appear in some form of 'continuum excitation'. The energy density including only 'formed' hadrons (during the expansion of the system) stays below 1 GeV/fm^3 , i.e. below the energy density expected for a transition to the QGP. The absolute numbers in Fig. 14 have to be compared to the volume of a *Au*-nucleus in the moving frame which, for a Lorentz γ -factor of 3.78, gives $\approx 330 \text{ fm}^3$. Thus also at 25 A·GeV the phase boundary to a QGP might be probed in a sizeable volume for time scales of a few fm/c. Contrary to central collisions at the SPS these volumes are characterized by a high net quark density; for such configurations we presently have no guide from QCD lattice calculations.

The multiplicity of open charm mesons at 25 A·GeV is about $5 \cdot 10^{-4}$, whereas the multiplicity of J/Ψ 's (including the decay of χ_c) is about $1.5 \cdot 10^{-5}$. We mention that the fraction of charmonia dissociated by baryons and mesons is $\sim 60\%$ for J/Ψ [14].

The effect of rescattering of D -mesons on baryons and mesons is displayed in Fig. 15 (for a central collision of *Au + Au*) for the D -meson rapidity distribution, which shows now a substantial broadening due to scattering processes with baryons and mesons. The decrease of the D -meson rapidity distribution at midrapidity is almost a factor of 2.

The m_T -spectra for all mesons in analogy to Fig. 5 (for pp reactions) are presented in Fig. 16. The calculated m_T spectrum for pions, kaons, ϕ -mesons can be characterized by an exponential slope parameter of 143 MeV (dashed line). Again the kaon (and ϕ) yield is increased (relative to pp times the number of hard collisions N_{coll}) due to rescattering (cf. Fig. 13), but the ϕ ($s\bar{s}$) mesons stay down by a factor of 3-4. The charmonium spectrum (relative to pp) is decreased by a factor ≈ 2.5 due to dissociation as noted before and approximately fulfills the global m_T -scaling. The latter does not hold for D -mesons (open squares) which are suppressed dynamically in the threshold region by roughly one order of magnitude.

We recall that a similar observation has been made for the m_T -scaling of K^+ and K^- mesons close to threshold energies at the SIS [72], where the strange mesons have been suppressed relative to pions and η 's. However, when adding to the K^+ mass the $\Lambda - N$ mass difference of 177 MeV (due to the associated production mechanism in pp and πN collisions), a remarkable m_T -scaling could be recovered again [72]. It should be noted that the latter scaling is not due to a grand-canonical chemical equilibration, but simply due to a shift of the spectra induced by the kaon production mechanism. We have to stress, however, that all these observations on the charm sector are based on our extrapolations (Section 2) and might not hold experimentally.

We now address the question, to what extent in-medium modifications of the D -mesons might be seen in the m_T -spectra for central *Au + Au* collisions at 25 A GeV. Contrary to open charm production and propagation in antiproton induced reactions on nuclei [26], where the D -mesons show up with momenta of a couple of GeV/c relative to the nuclear matter rest frame, the D -mesons produced in central nucleus-nucleus collisions have only small momenta in the rest frame of the hadronic fireball. This is of particular relevance for experimental studies of hadron self energies, since the latter are generally momentum dependent and most pronounced for low momenta.

The modifications of the D -meson spectral functions in the medium at present cannot be reliably calculated nor extracted (in the low density limit) from experimental scattering

data via a dispersion analysis (cf. Ref. [73] for the K, \bar{K} problem). For our initial study we thus discard all momentum dependence of the D -meson self energies and also neglect a broadening of their spectral functions due to interactions in the medium. As a guide we employ the QCD sum rule calculations from Ref. [27] and implement a mass shift of the form

$$\Delta m_D(\rho) = \alpha_D \frac{\rho}{\rho_0} \quad (9)$$

with $\alpha_D \approx -50$ MeV, where ρ_0 denotes the nuclear matter density and ρ the actual baryon density at the D -meson creation point. Since the c, \bar{c} pairs are created in the early high density phase of the collision and baryon densities up to $8\rho_0$ can be achieved in central $Au + Au$ collisions at 25 A GeV, the D -meson mass shifts in this case reach up to -400 MeV. Such mass shifts have a dramatic effect on the production cross sections in pN collisions when incorporating them in the production thresholds (cf. Tables 1 and 2).

Our calculations with the mass shift (9) give an enhancement of the D -meson yield by about a factor of 7 relative to the bare-mass case. The slope of the spectra is not reduced very much due to elastic scattering with (dominantly) pions as can be seen from Fig. 16 for the resulting m_T spectrum (crosses). Somewhat surprisingly, an approximate m_T -scaling with all other mesons is regained in this case. We have to point out again that the results on open charm and charmonia in Fig. 16 essentially depend on our extrapolations in Section 2 and the assumed self energies (9), which are not controlled by data. On the other hand, Fig. 16 should be helpful in guiding the experimental analysis. For a direct comparison of the calculated m_T -spectra with experiment, however, the final state elastic rescattering processes of kaons and ϕ -mesons with pions have to be included which lead to similar modifications of the slope parameters as discussed at the end of Section 3.1.

3.3 Excitation functions of mesons in central collisions

In order to provide an overview on meson production we show in Fig. 17 the excitation function of open charm mesons in central $Au + Au$ collisions from AGS to RHIC energies without employing any self energies for these mesons. The D -mesons with a \bar{c} are produced more frequently at low energies due to the associated production with $\Lambda_c, \Sigma_c, \Sigma_c^*$ similar to the kaon case (cf. lower part). At roughly 15 A·GeV the cross sections for open charm and charmonia are similar, while the ratio of open charm to charmonia bound states increases rapidly with energy. This behaviour is quite similar to the excitation functions in the strangeness sector when comparing K^+, K^- and ϕ -mesons. Since the excitation function for open charm drops very fast with decreasing bombarding energy, experiments around 20 A·GeV will be a challenging task since the multiplicity of the other mesons is higher by orders of magnitude. On the other hand, the perspectives for open charm measurements at RHIC appear promising since about 15 $c\bar{c}$ (or $D\bar{D}$) pairs should be created in central $Au + Au$ collisions according to our calculations.

We mention that the excitation functions for the pions, kaons, eta's and ϕ -mesons have been taken from Ref. [14], while the multiplicities for J/Ψ have been recalculated using the novel comover absorption cross sections from Section 2 and Ref. [16] as well the parametrization (2) instead of the Schuler fit [48]. Since the numbers up to 500 A·GeV

are compatible within 30% we do not discuss these differences in more detail. The higher J/Ψ multiplicity at RHIC energies is a direct consequence of the cross section (2).

4 Summary

In this work we have calculated excitation functions for open charm mesons in central $Au + Au$ reactions from AGS to RHIC energies within the HSD transport approach. We have switched off elastic final state interactions of kaons and ϕ -mesons with pions in order to suppress their common acceleration in the 'pion wind' during the expansion phase. The 'input' open charm cross sections from pp and πN reactions have been fitted to results from PYTHIA and scaled in magnitude to the available experimental data. Within these parametrizations and results from the LUND string model [50] – which is incorporated in the HSD approach – we find an m_T -scaling for pions, kaons, D -mesons and J/Ψ in central collisions of $Au + Au$ at the SPS (with an apparent slope of 176 MeV) without employing the assumption of a Quark-Gluon Plasma (QGP). We have shown that this result is essentially due to an approximate m_T -scaling in pp collisions at $\sqrt{s} = 17.3$ GeV and D, \bar{D} and J/Ψ final state interactions.

At bombarding energies of 25 A·GeV a suppression of D -mesons by a factor of ~ 10 relative to a global m_T -scaling with a slope of 143 MeV is expected if no D -meson self energies are accounted for. On the other hand, attractive mass shifts of -50 MeV at ρ_0 – when extrapolated linearly in the baryon density – lead to an enhancement of open charm mesons by about a factor of 7 such that an approximate m_T -scaling for all mesons (cf. Fig. 16) is regained. However, as pointed out throughout this work, the elementary cross sections for open charm and charmonia have to be measured in the relevant kinematical regimes before reliable conclusions can be drawn in the nucleus-nucleus case. Experimental data in the 20 - 30 A·GeV with light and heavy systems will have to clarify, furthermore, if the quasi-particle picture of open charm mesons at high baryon density is applicable at all.

Acknowledgements

The authors are grateful to C. Greiner for helpful discussions and to P. Senger for valuable suggestions.

References

- [1] *Quark Matter '96*, Nucl. Phys. A 610 (1996) 1.
- [2] *Quark Matter '97*, Nucl. Phys. A 638 (1998) 1.
- [3] *Quark Matter '99*, Nucl. Phys. A 661 (1999) 1.
- [4] *Strangeness in Quark Matter 1998*, J. Phys. G 25 (1999) 143.
- [5] U. Heinz, Nucl. Phys. A 661 (1999) 140c.

- [6] T. Matsui, H. Satz, Phys. Lett. B 178 (1986) 416.
- [7] H. Satz, Rep. Progr. Phys. 63 (2000) 1511.
- [8] M. C. Abreu et al., NA50 collaboration, Phys. Lett. B 477 (2000) 28.
- [9] M. C. Abreu et al., NA50 collaboration, Phys. Lett. B 450 (2000) 456.
- [10] W. Cassing, E. L. Bratkovskaya, Phys. Rep. 308 (1999) 65.
- [11] R. Vogt, Phys. Rep. 310 (1999) 197.
- [12] C. Gerschel, J. Hüfner, Ann. Rev. Nucl. Part. Sci. 49 (1999) 255.
- [13] X.N. Wang, B. Jacak, eds., *Quarkonium Production in High-Energy Nuclear Collisions*, World Scientific 1998.
- [14] W. Cassing, E. L. Bratkovskaya, S. Juchem, Nucl. Phys. A 674 (2000) 249.
- [15] A. Capella, E. G. Ferreira, A. B. Kaidalov, Phys. Rev. Lett. 85 (2000) 2080.
- [16] K. L. Haglin, Phys. Rev. C 61 (2000) 031903.
- [17] K. L. Haglin, C. Gale, nucl-th/0010017.
- [18] Z. Lin, C. M. Ko, Phys. Rev. C 62 (2000) 034903.
- [19] Z. Lin, C. M. Ko, nucl-th/0008050.
- [20] A. Sibirtsev, K. Tsushima, A. W. Thomas, nucl-th/0005041.
- [21] A. Sibirtsev, K. Tsushima, K. Saito, A. W. Thomas, Phys. Lett. B 484 (2000) 23.
- [22] B. Müller, Nucl. Phys. A 661 (1999) 272c.
- [23] M. C. Abreu et al., NA50 collaboration, Eur. Phys. J. C 14 (2000) 443.
- [24] Review of Particle Physics, Eur. Phys. J. C 15 (2000) 1.
- [25] G. Q. Li, G. E. Brown, Nucl. Phys. A 636 (1998) 487; Phys. Rev. C 58 (1998) 1698.
- [26] A. Sibirtsev, K. Tsushima, A. W. Thomas, Eur. Phys. J. A 6 (1999) 351.
- [27] A. Hayashigaki, Phys. Lett. B 487 (2000) 96.
- [28] F. Klingl, S. Kim, S. H. Lee, P. Morath, W. Weise, Phys. Rev. Lett. 82 (1999) 3396.
- [29] P. Braun-Munzinger, J. Stachel, nucl-th/0007059.
- [30] P. Braun-Munzinger, D. Miskowiec, A. Dress, C. Lourenco, Eur. Phys. J. C 1 (1998) 123.
- [31] R. L. Thews, M. Schroedter, J. Rafelski, hep-ph/0007323.

- [32] Z. Lin, X.-N. Wang, Phys. Lett. B444 (1998) 245.
- [33] Z. Lin, C. M. Ko, B. Zhang, Phys. Rev. C 61 (2000) 024904.
- [34] Proposal CERN/SPSC 2000-010.
- [35] M. Gazdzicki, C. Markert, Acta Phys. Polon. B 31 (2000) 965.
- [36] H.-U. Bengtsson, T. Sjöstrand, Comp. Phys. Commun. 46 (1987) 43.
- [37] M. Aguilar-Benitez et al., Phys. Lett. B 135 (1984) 237.
- [38] M. Aguilar-Benitez et al., Z. Phys. C 40 (1988) 321.
- [39] R. Ammar et al., Phys. Rev. Lett 61 (1988) 2185.
- [40] K. Kodama et al., Phys. Lett. B 284 (1992) 461.
- [41] M. J. Leitch et al., Phys. Rev. Lett. 72 (1994) 2542.
- [42] S. Barlag et al., Z. Phys. C 49 (1991) 555; Phys. Lett. B 247 (1990) 113.
- [43] K. Kodama et al., Phys. Lett. B 263 (1991) 573.
- [44] S. Barlag et al., Z. Phys. C 39 (1988) 451.
- [45] G. A. Alves et al., Phys. Rev. Lett. 77 (1996) 2388; *ibid.* 2392.
- [46] M. Adamovich et al., Nucl. Phys. B 495 (1997) 3.
- [47] E. M. Aitala et al., Eur. Phys. J. C 4 (1999) 1.
- [48] G. A. Schuler, CERN preprint, CERN-TH 7170/94.
- [49] J. Geiss, W. Cassing, C. Greiner, Nucl. Phys. A 644 (1998) 107.
- [50] B. Anderson, G. Gustafson, Hong Pi, Z. Phys. C 57 (1993) 485.
- [51] H. Plochow-Besch, Int. J. Mod. Phys. A 10 (1995) 2901.
- [52] S. Frixione, M. L. Mangano, P. Nason, G. Ridolfi, hep-ph/9702287.
- [53] R. Vogt, Atomic Data and Nuclear Data Tables 50 (1992) 343.
- [54] F. Becattini, Z. Phys. C 69 (1996) 485.
- [55] W. F. Henning, P. Senger, priv. communication.
- [56] W. Cassing, E. L. Bratkovskaya, Nucl. Phys. A 623 (1997) 570.
- [57] J. Geiss, C. Greiner, E. L. Bratkovskaya, W. Cassing, U. Mosel, Phys. Lett. B 447 (1999) 31.

- [58] J. Formanek, Nucl. Phys. B12 (1969) 59.
- [59] W. Szyz and L.C. Maximon, Ann. Phys. 52 (1969) 59.
- [60] J. O. Schmitt, G. C. Nayak, H. Stöcker, W. Greiner, hep-ph/0009258.
- [61] D. Kharzeev, R. L. Thews, Phys. Rev. C 60 (1999) 041901.
- [62] P. Braun-Munzinger, K. Redlich, Eur. Phys. J. C 16 (2000) 519.
- [63] E. L. Bratkovskaya et al., Nucl. Phys. A 675 (2000) 661.
- [64] W. Cassing, C. M. Ko, Phys. Lett. B 396 (1997) 39.
- [65] M. Gazdzicki, M. Gorenstein, Phys. Rev. Lett. 83 (1999) 4009.
- [66] M. Gazdzicki, Phys. Rev. C 60 (1999) 054903.
- [67] K. Gallmeister, B. Kämpfer, O. P. Pavlenko, Phys. Lett. B 473 (2000) 20.
- [68] R. Stock, Nucl. Phys. A 661 (1999) 282c.
- [69] C. A. Ogilvie for the E866 and E819 Collaboration, Nucl. Phys. A 638 (1998) 57c;
J. Phys. G 25 (1999) 159.
- [70] F. Karsch, Nucl. Phys. B (Proc. Suppl.) 83-84 (2000) 14.
- [71] P. K. Sahu, W. Cassing, U. Mosel, A. Ohnishi, Nucl. Phys. A 672 (2000) 376.
- [72] E. L. Bratkovskaya, W. Cassing, U. Mosel, Phys. Lett. B 424 (1998) 244 .
- [73] A. Sibirtsev, W. Cassing, Nucl. Phys. A 641 (1998) 476.

Table 1: The parameters a_x, α and β for pN reactions

pN				
Meson	$\sqrt{s_0}$ [GeV]	a_x [mb]	α	β
D^0	5.605	0.523	4.92	1.36
\bar{D}^0	5.069	0.496	4.96	1.36
D^+	5.609	0.469	4.76	1.40
D^-	5.073	0.363	4.94	1.44
D^{0*}	5.889	1.775	4.90	1.34
\bar{D}^{0*}	5.230	1.275	4.56	1.42
D^{+*}	5.896	1.514	4.64	1.40
D^{-*}	5.233	1.384	5.20	1.36
D_s^+	5.813	0.171	5.12	1.34
D_s^-	5.373	0.102	5.58	1.42
D_s^{+*}	6.101	0.496	4.88	1.38
D_s^{-*}	5.516	0.283	5.50	1.46

Table 2: The parameters a_x, α and β for πN reactions

πN				
Meson	$\sqrt{s_0}$ [GeV]	a_x [mb]	α	β
D^0	4.667	0.273	2.86	1.28
\bar{D}^0	4.150	0.247	3.80	1.26
D^+	4.671	0.255	3.22	1.28
D^-	4.154	0.286	3.50	1.22
D^{0*}	4.951	1.076	3.14	1.22
\bar{D}^{0*}	4.292	0.774	3.80	1.26
D^{+*}	4.955	0.719	2.86	1.32
D^{-*}	4.296	0.839	3.40	1.24
D_s^+	4.875	0.0932	3.62	1.22
D_s^-	4.435	0.0545	3.70	1.34
D_s^{+*}	5.162	0.284	3.42	1.24
D_s^{-*}	4.578	0.163	3.64	1.34

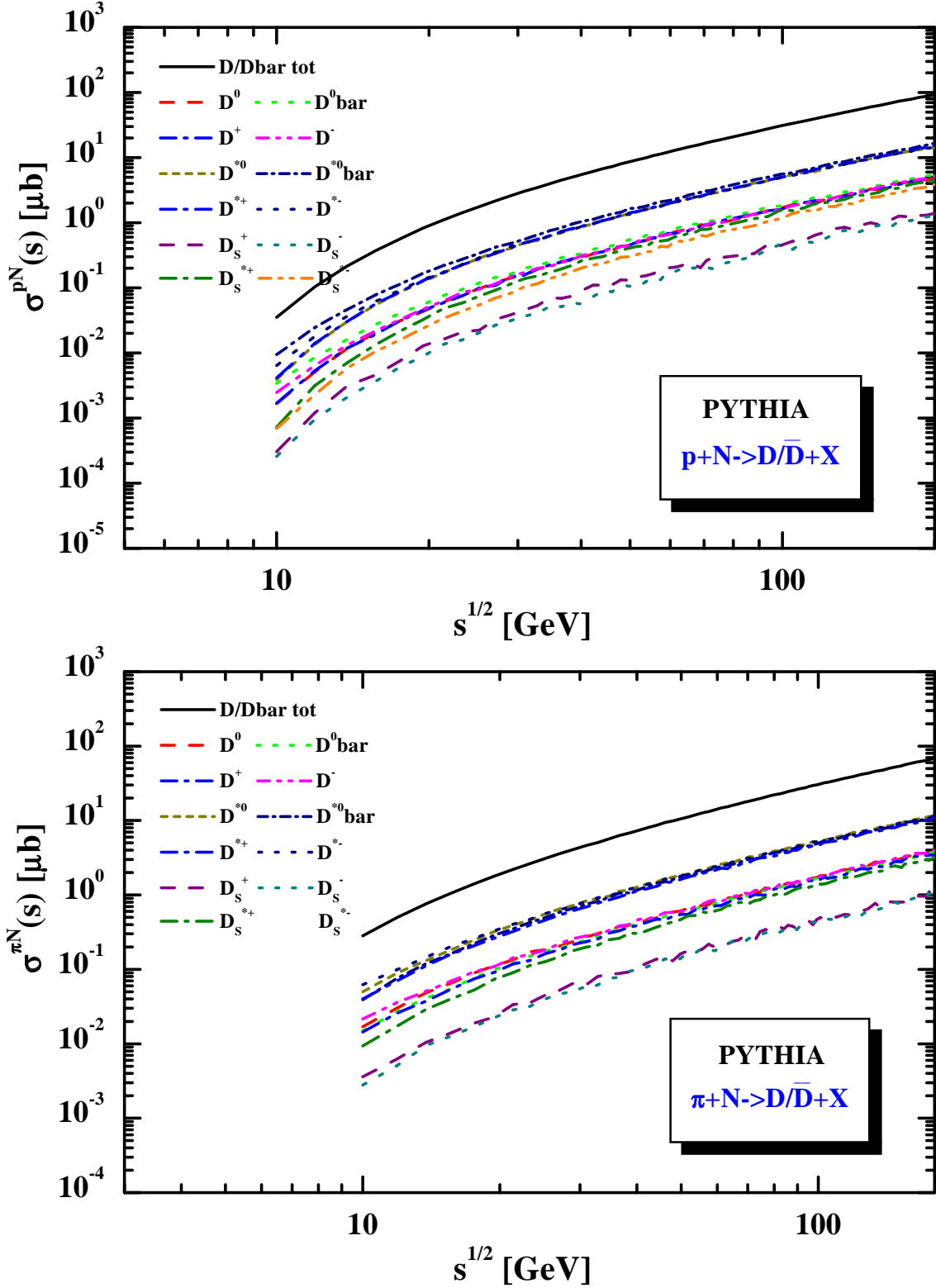


Figure 1: The cross section for open charm mesons from PYTHIA [36] for pp (upper part) and πN reactions (lower part) using MRS G structure functions, $m_c = 1.5$ GeV and $k_T = 1$ GeV, respectively. The upper solid lines denote the sum over all $D + \bar{D}$ mesons.

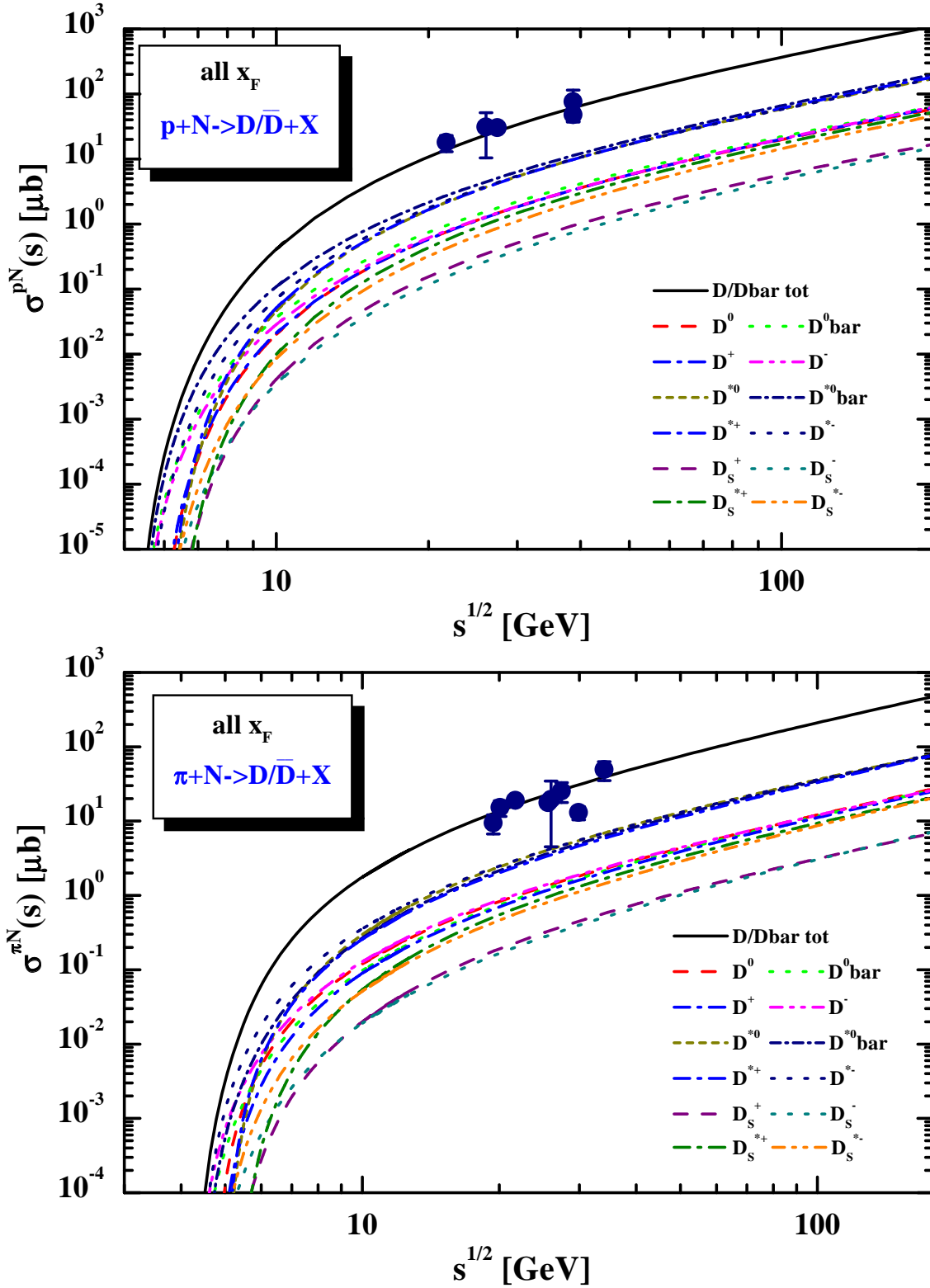


Figure 2: The cross section for open charm mesons in the parametrization (1) using the parameters from Tables 1 and 2 in comparison to the experimental data from Refs. [37]–[47] for pp (upper part) and πN reactions (lower part). The upper solid lines denote the sum over all $D + \bar{D}$ mesons.

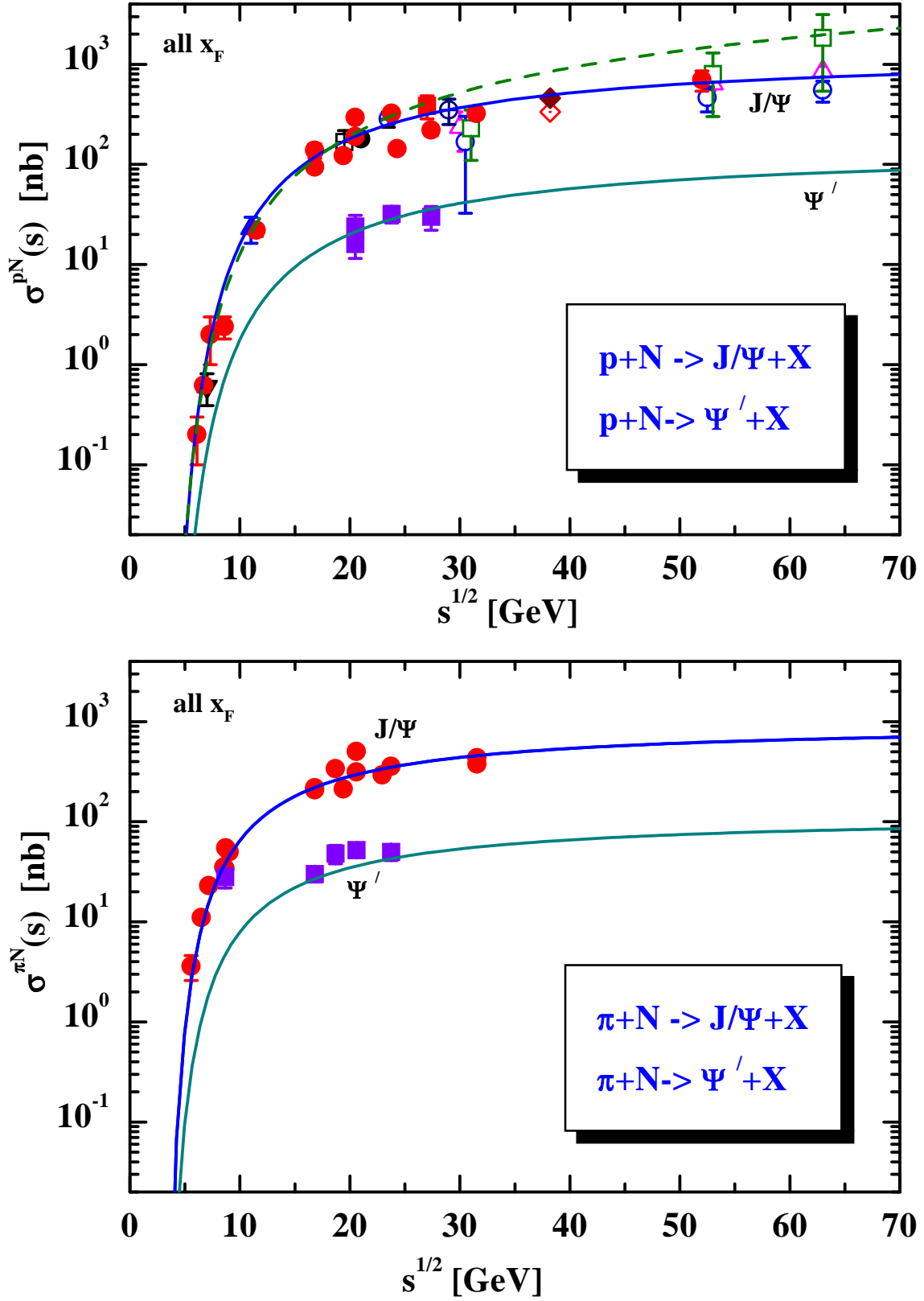


Figure 3: The cross section for J/Ψ and Ψ' mesons in the parametrizations from Ref. [48] (solid lines) in comparison to the experimental data for pN (upper part) and πN reactions (lower part). The J/Ψ cross sections include the decay from χ_c mesons. The dashed line in the upper part shows the J/Ψ cross section for the parametrization (2).

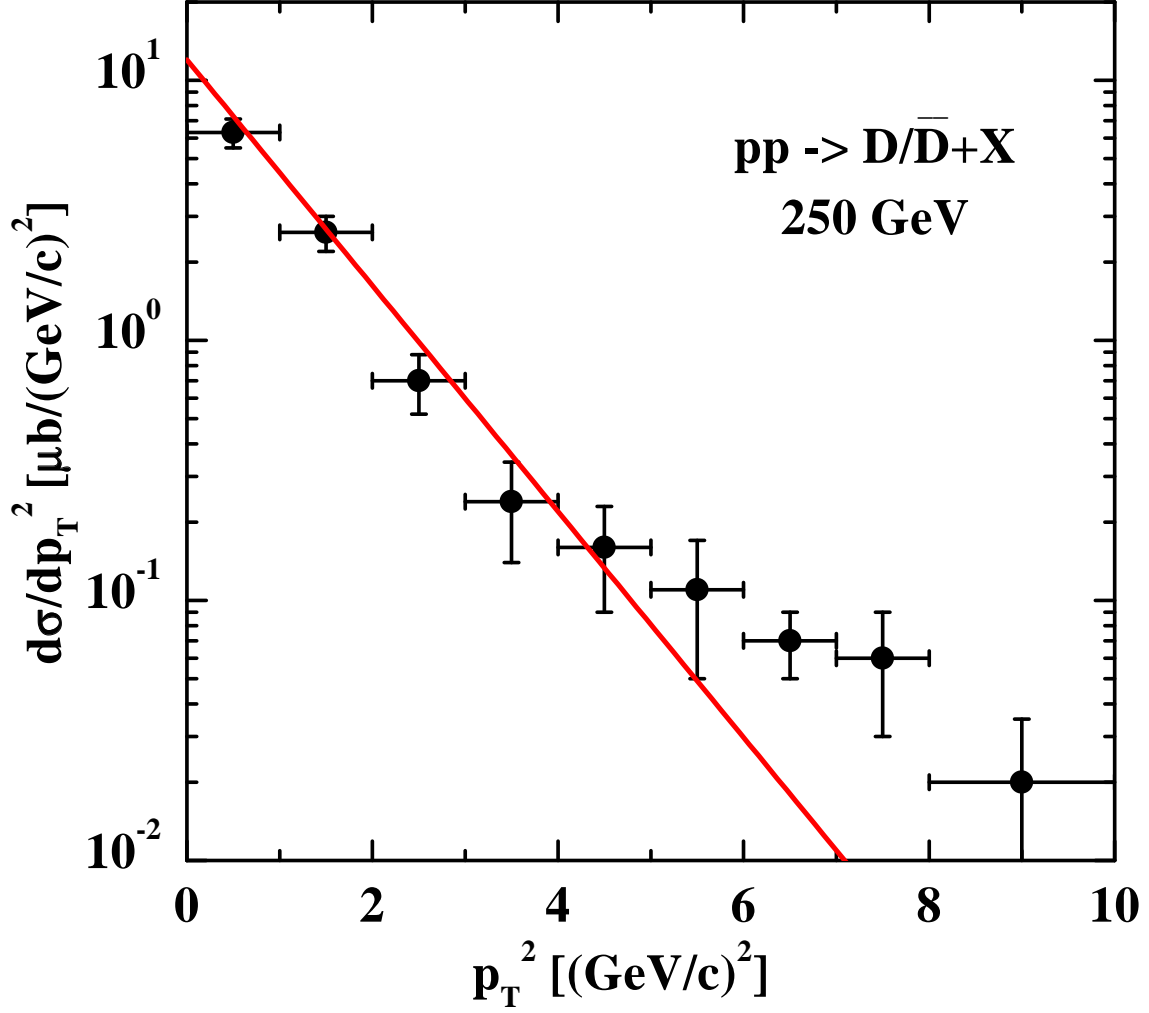


Figure 4: The differential cross section for D/\bar{D} mesons in transverse momentum (squared) for pp reactions at 250 GeV within the parametrisation (3) (solid line) in comparison to the data from Ref. [45].

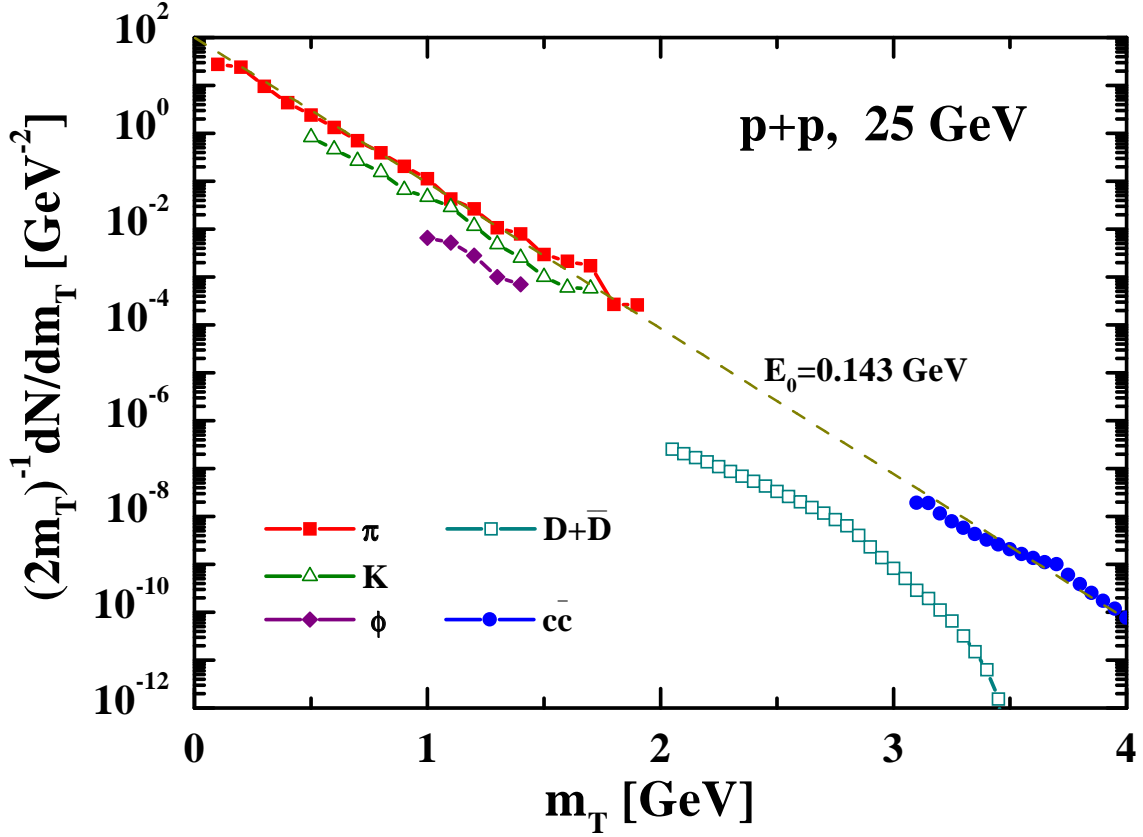


Figure 5: The transverse mass spectra from pp collisions at $T_{lab} = 25$ GeV for pions (full squares), kaons (open triangles), and ϕ -mesons (full rhombes) from the LUND string model [50] as implemented in HSD. The $D + \bar{D}$ meson (open squares) and charmonium (full dots) spectra – including the decay $\chi_c \rightarrow J/\Psi + \gamma$ – result from the parametrizations specified in Section 2. The dashed line shows an exponential with slope parameter $E_0 = 0.143$ GeV.

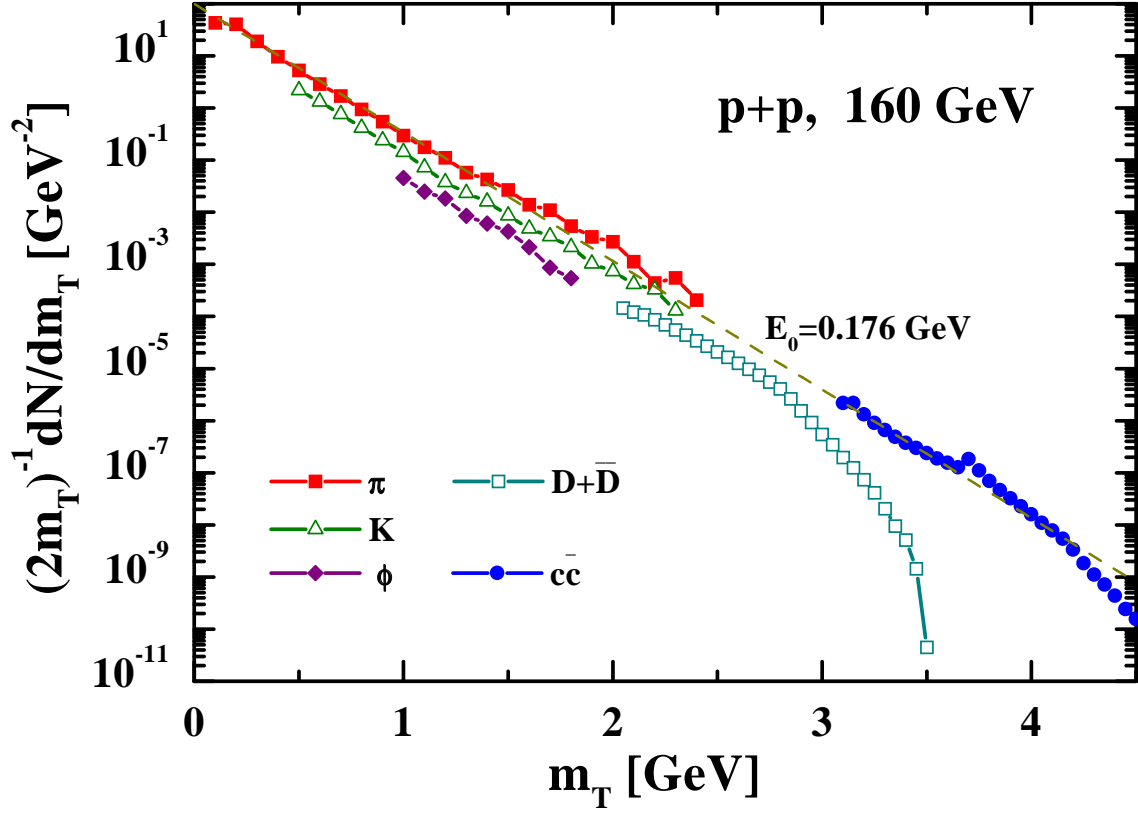


Figure 6: Same as Fig. 5 for pp reactions at $T_{lab} = 160 \text{ GeV}$. The dashed line shows an exponential with slope parameter $E_0 = 0.176 \text{ GeV}$.

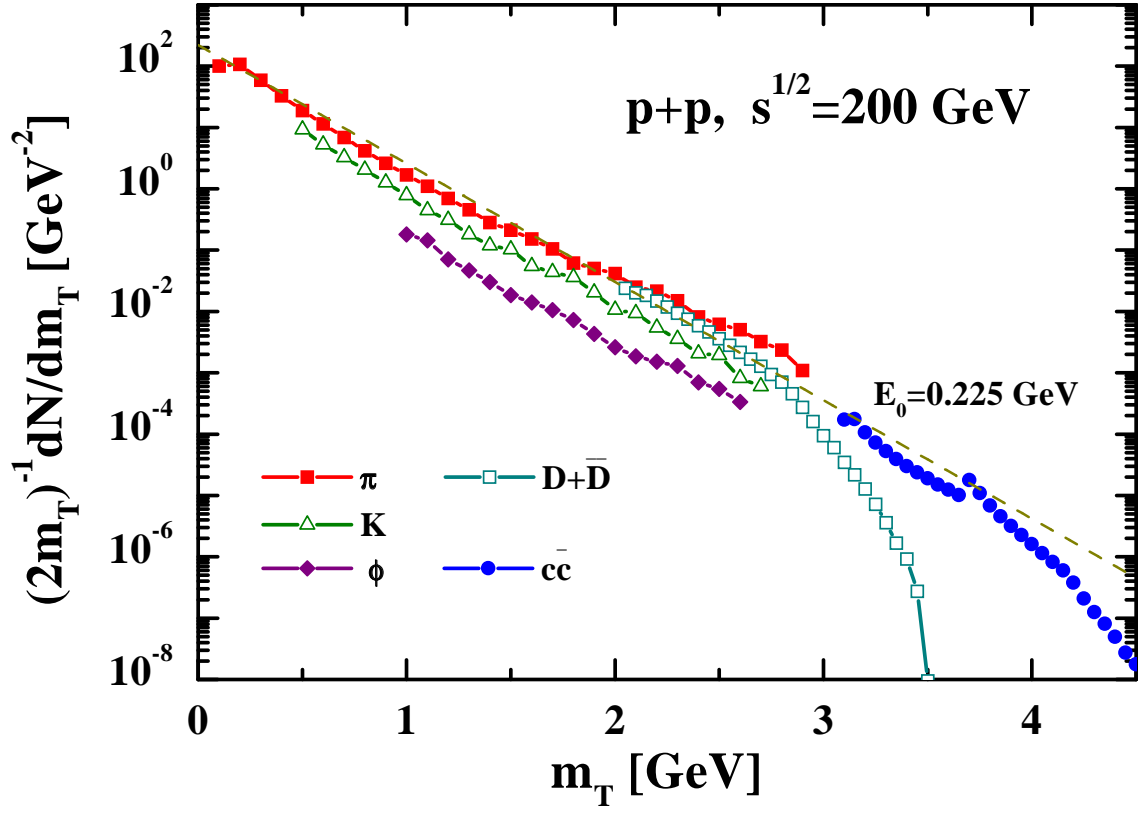


Figure 7: Same as Fig. 5 for pp reactions at $\sqrt{s} = 200$ GeV. The dashed line shows an exponential with slope parameter $E_0 = 0.225$ GeV.

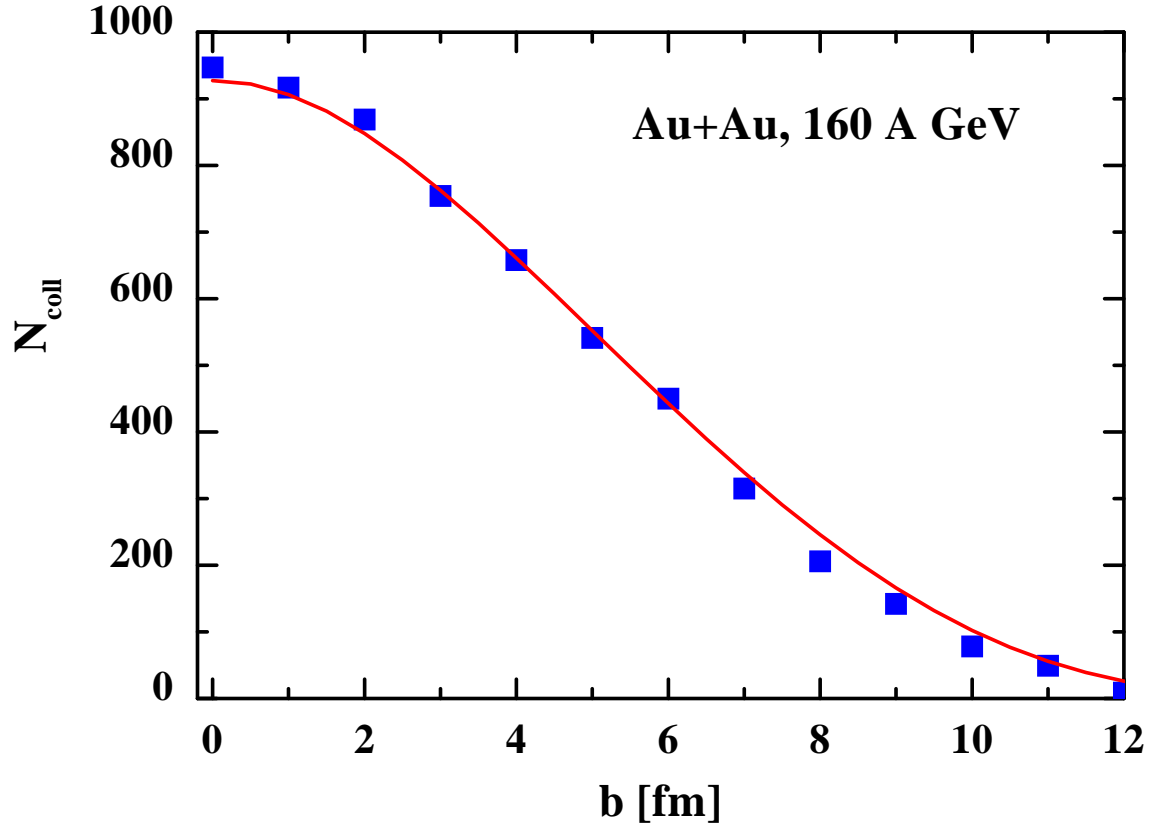


Figure 8: The number of hard collisions N_{coll} as a function of impact parameter b in the HSD approach (full squares) for $Au + Au$ at 160 A·GeV (see text) in comparison to the number of collisions in the Glauber approach (solid line).

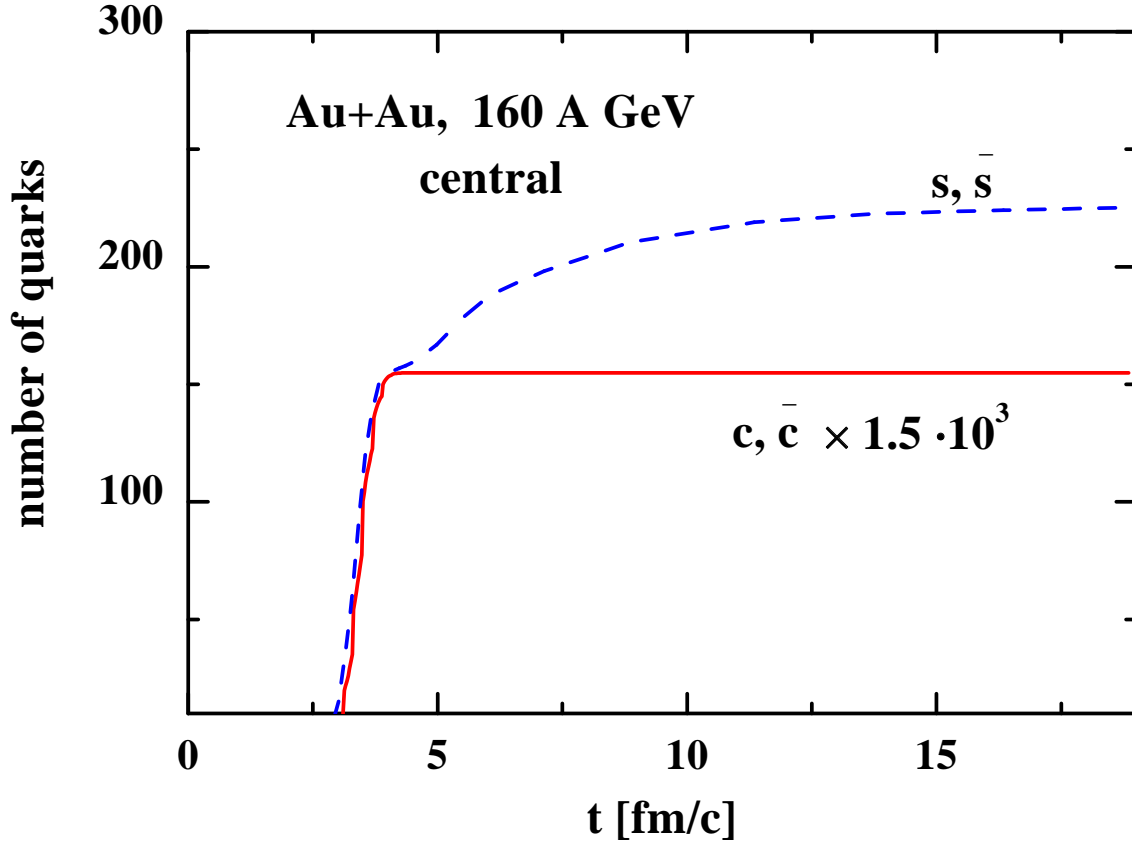


Figure 9: Time evolution for the production of s, \bar{s} (dashed line) and $c\bar{c}$ quarks (solid line, multiplied by a factor of 1.5×10^3) in the HSD approach for a central $Au + Au$ reaction at 160 A·GeV. The c, \bar{c} numbers have been scaled to the initial hard scattering processes.

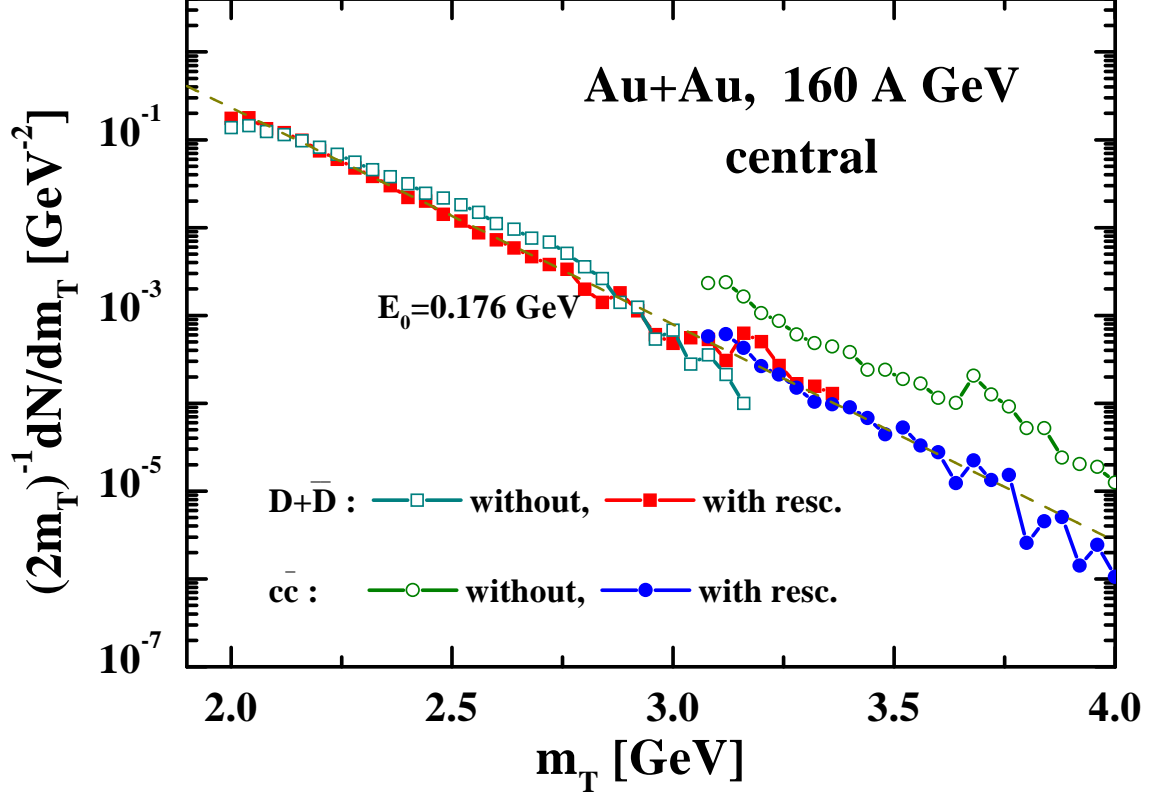


Figure 10: The transverse mass spectra of $D + \bar{D}$ mesons and $J/\Psi, \Psi'$ mesons in the HSD approach for a central $Au + Au$ collision at 160 A·GeV. The open symbols denote the spectra without rescattering and reabsorption while the full symbols include the final state interactions. The thin dashed line shows an exponential with slope parameter $E_0 = 0.176 \text{ GeV}$.

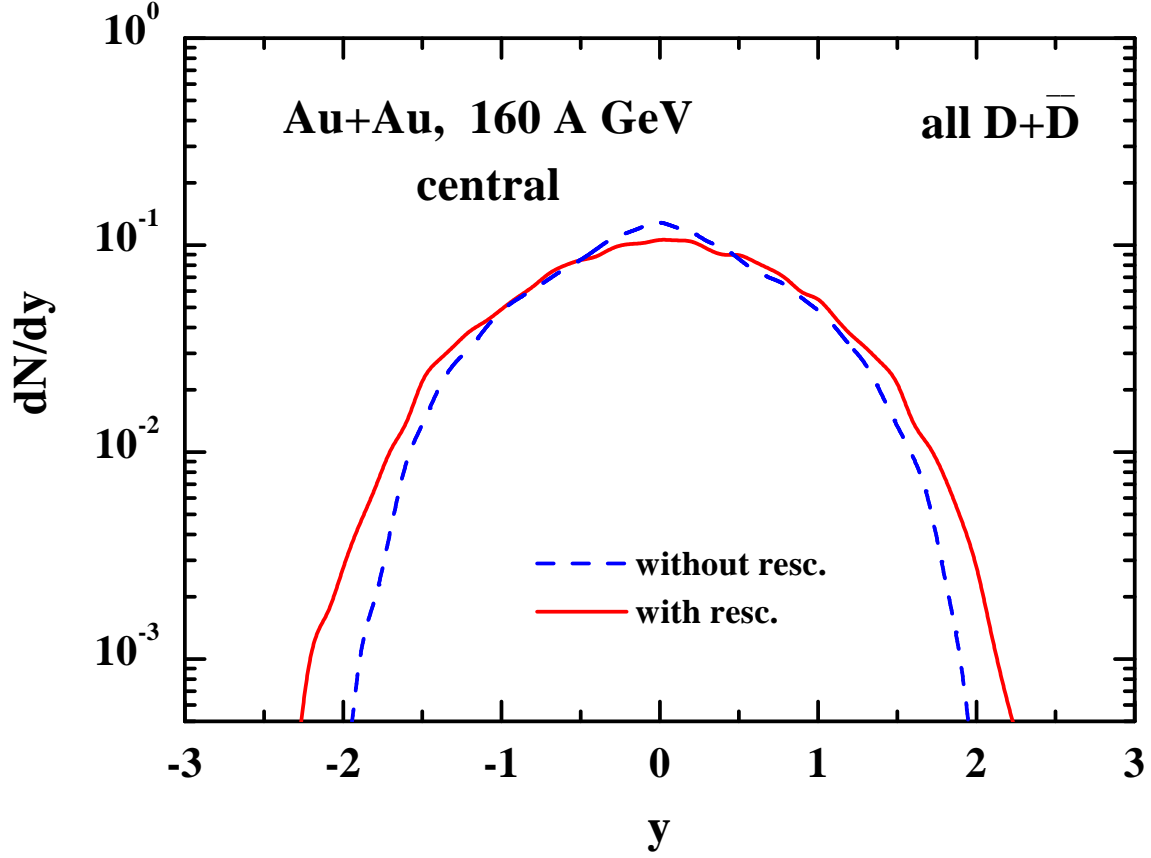


Figure 11: The rapidity distribution of $D + \bar{D}$ mesons in the HSD approach for a central $Au + Au$ collision at 160 A·GeV. The dashed line denotes the spectrum without rescattering and reabsorption while the solid line includes the final state interactions of D -mesons with hadrons.

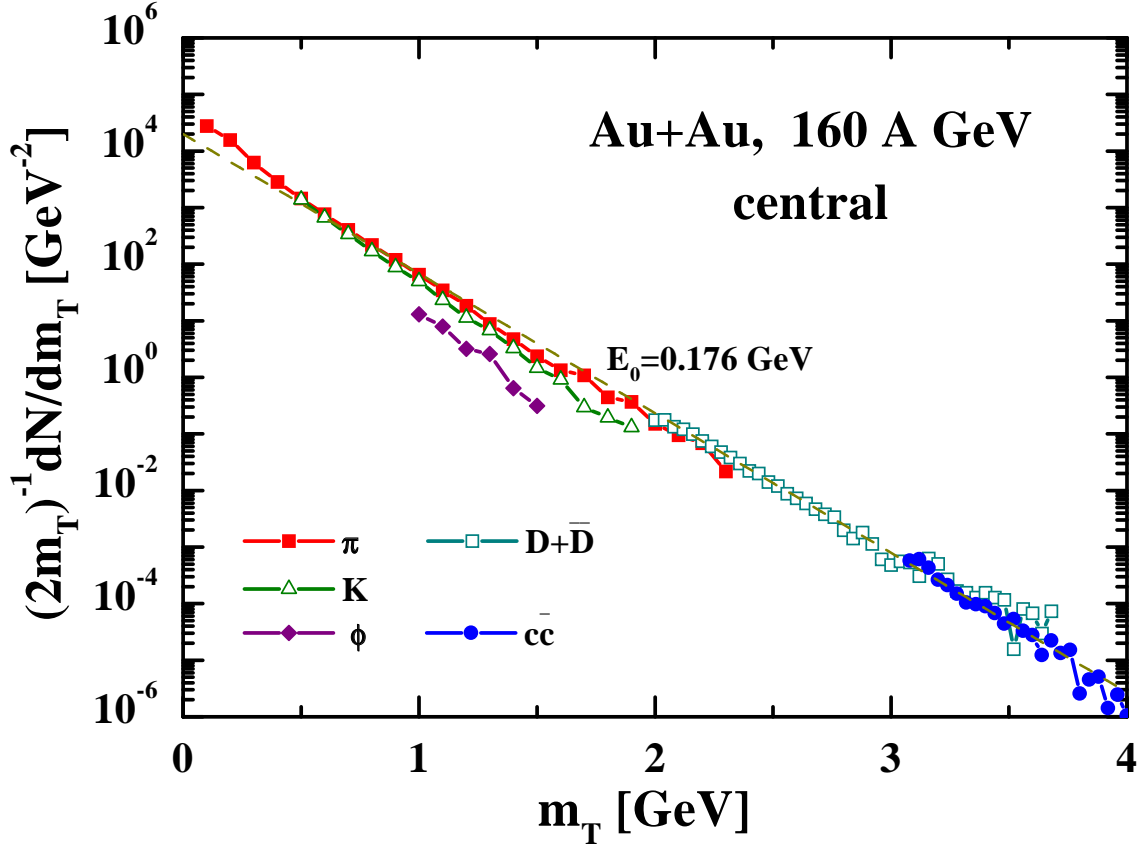


Figure 12: The transverse mass spectra of pions (full squares), kaons (open triangles), ϕ -mesons (full rhombes), $D + \bar{D}$ mesons (open squares) and $J/\Psi, \Psi'$ mesons (full dots) in the HSD approach for a central $Au + Au$ collision at 160 A·GeV. The thin dashed line shows an exponential with slope parameter $E_0 = 0.176 \text{ GeV}$. Note that final state elastic scattering of kaons and ϕ -mesons with pions has been discarded in the calculations.

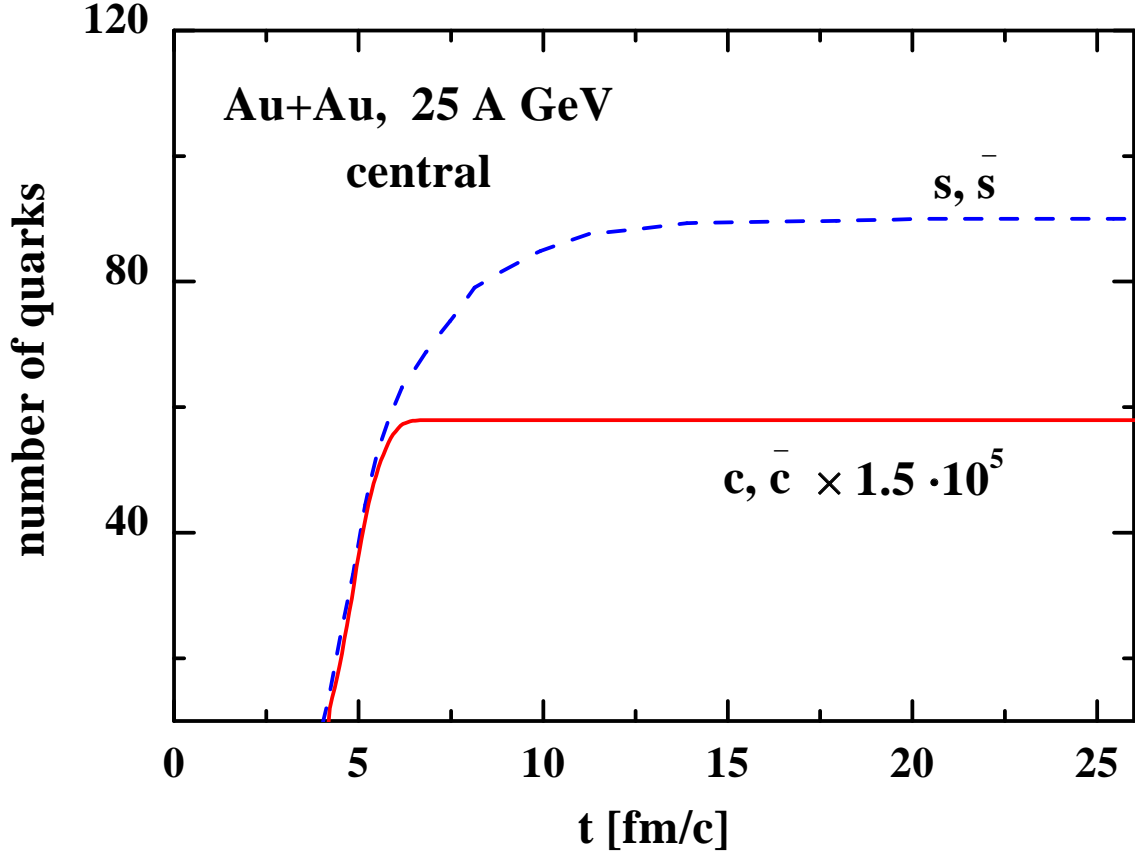


Figure 13: Time evolution for the production of s, \bar{s} (dashed line) and $c\bar{c}$ quarks (solid line) in the HSD approach for a central $Au + Au$ reaction at 25 A·GeV. The c, \bar{c} numbers have been scaled to the initial hard scattering processes by a factor of 1.5×10^5 .

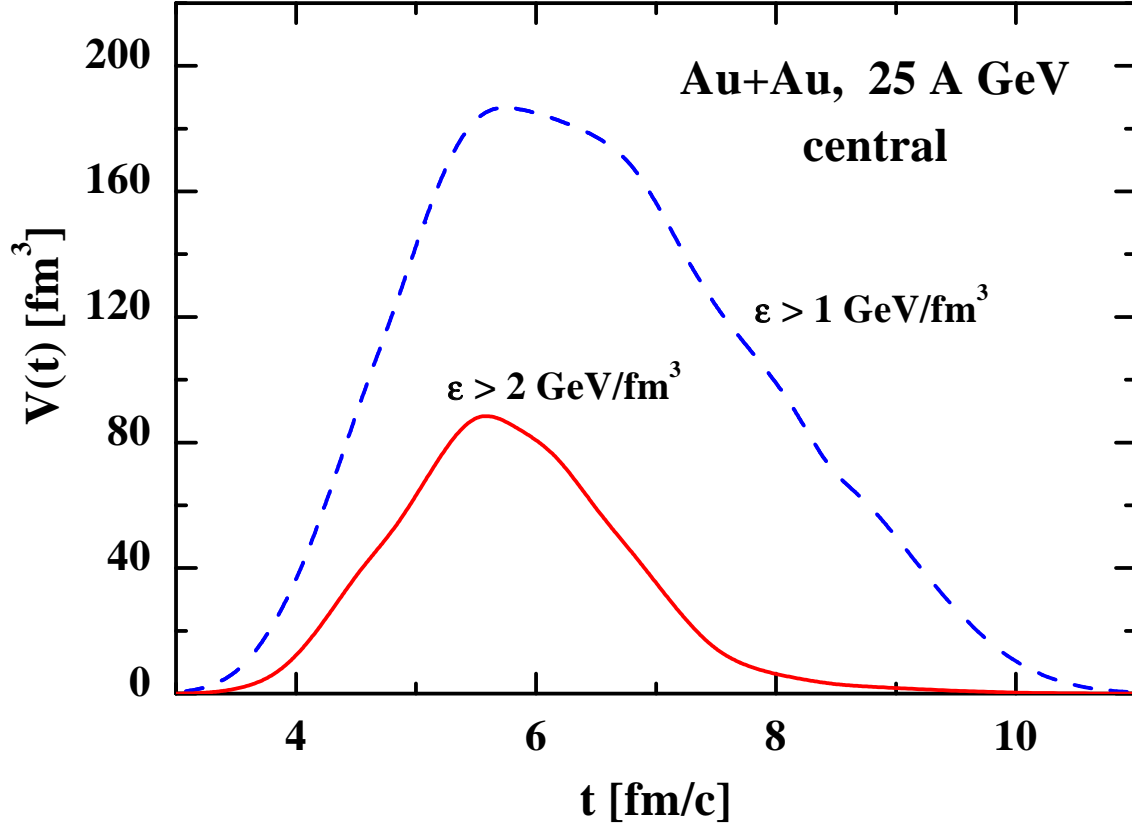


Figure 14: Time evolution for the volume with energy density $\epsilon \geq 1 \text{ GeV/fm}^3$ (dashed line) and $\geq 2 \text{ GeV/fm}^3$ (solid line) in the HSD approach for a central $Au + Au$ reaction at 25 A·GeV.

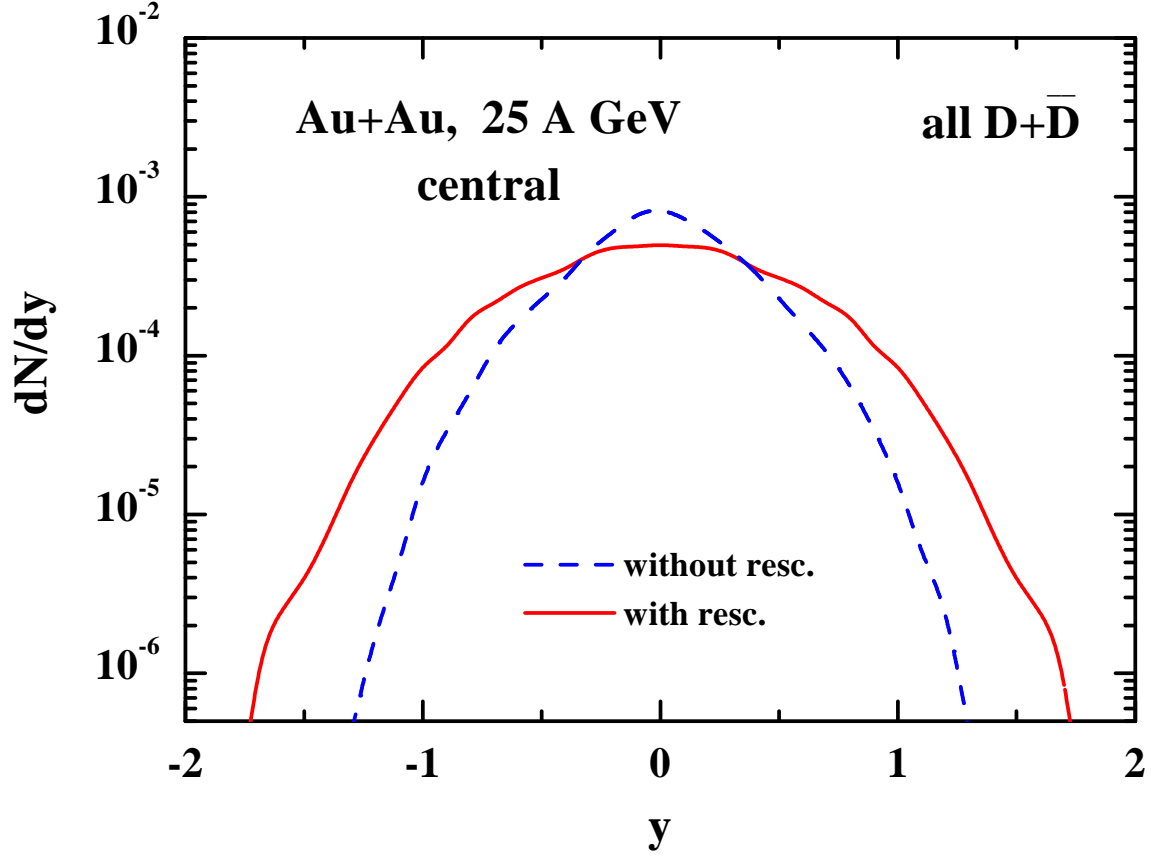


Figure 15: The rapidity distribution of $D + \bar{D}$ mesons in the HSD approach for a central $Au + Au$ collision at 25 A·GeV. The dashed line denotes the spectrum without rescattering while the solid line includes the final state interactions of D -mesons with hadrons.

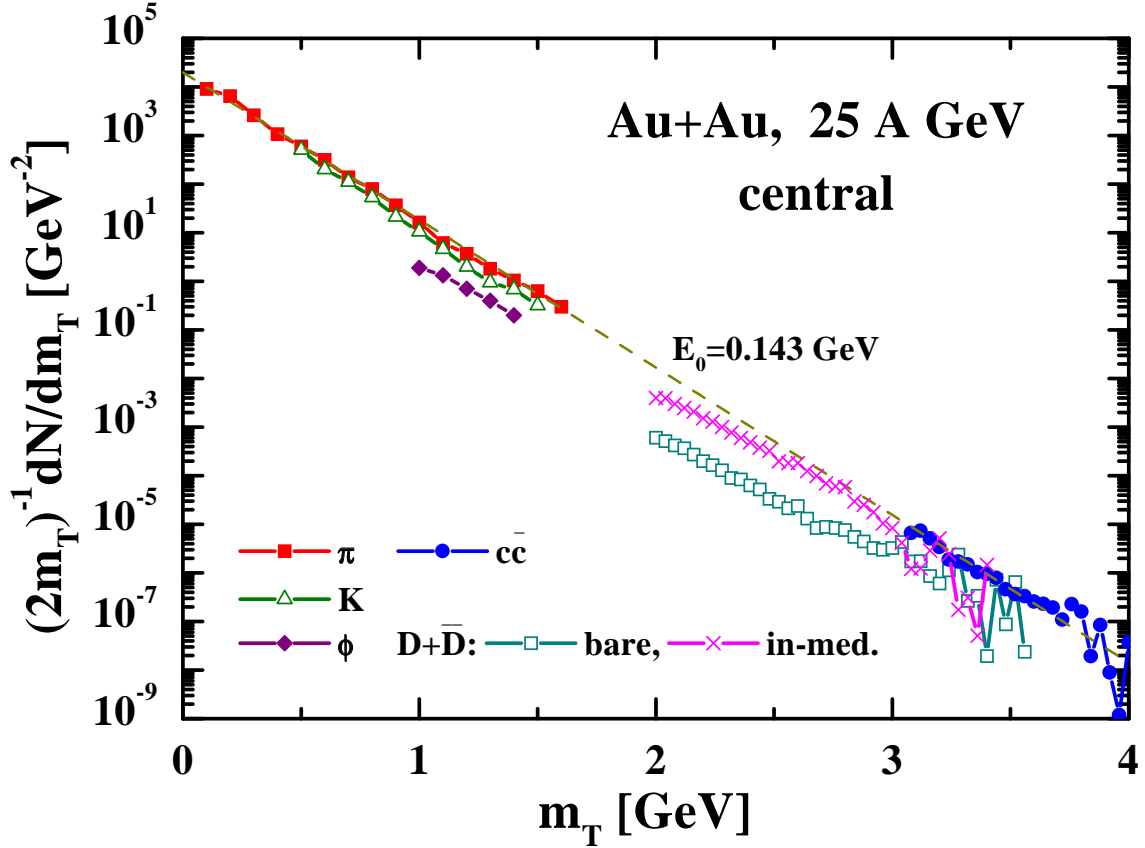


Figure 16: The transverse mass spectra of pions (full squares), kaons (open triangles), ϕ -mesons (full rhombes), $D + \bar{D}$ mesons (open squares) and $J/\Psi, \Psi'$ mesons (full dots) in the HSD approach for a central $Au + Au$ collision at 25 A·GeV without including self energies for the mesons. The crosses stand for the D -meson m_T spectra when including an attractive mass shift according to (9). The thin dashed line shows an exponential with slope parameter $E_0 = 0.143 \text{ GeV}$. Note that final state elastic scattering of kaons and ϕ -mesons with pions has been discarded in the calculations.

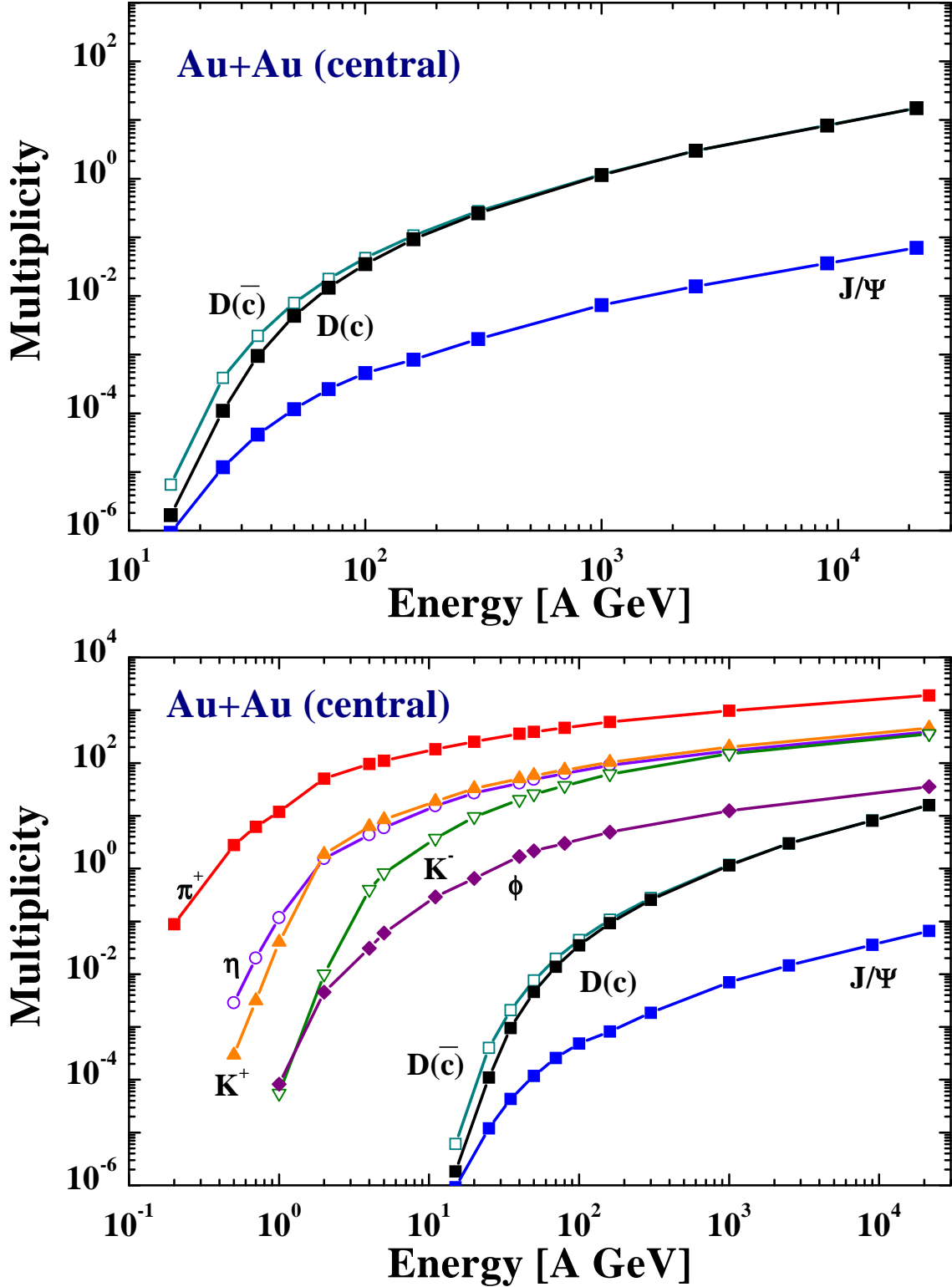


Figure 17: The multiplicity of D , \bar{D} and J/Ψ -mesons (upper part) for central collisions of $Au + Au$ in the HSD approach including elastic and inelastic reactions, but no in-medium modifications of their spectral functions. The multiplicities for π^+ , η , K^+ , K^- and ϕ (in the lower part) have been taken from Ref. [14] while the lines for $D(c)$, $D(\bar{c})$ and J/Ψ are the same as in the upper part.